2018 International Conference on Unmanned Aircraft Systems (ICUAS)
Dallas, TX, USA, June 12-15, 2018

Real-Time Guidance, Navigation and Control Framework for Fixed-Wing Aircraft Maneuvers in a Vertical Plane

Dilmurat Azimov *, Evan Kawamura †

Abstract. The goal of this study is to create a real-time guidance, navigation and control (GNC) framework for a fixed-wing aircraft (FWA) to perform various maneuvers in a vertical plane. This study offers a new approach for improving the FWA autonomy by enabling real-time sensor data fusion, targeting and re-targeting capabilities, new analytical/ numerical trajectory and attitude control solutions, and target-relative guidance. Existing FWA dynamical models are based on the traditional decoupling of their motion. This paper extends the utility of the concept of an instantaneous screw axis in guidance and control thereby promoting a new vision to general 6-degrees-of-freedom rigid body motion control. The existing flight vehicle guidance and control functions are mainly iterative and implicit, platform-specific, utilize pre-determined target states or way points, and executed typically utilizing the decoupled motion dynamical models. The research presented in this paper produces the GNC framework with the real-time target-relative guidance system, which is explicit and free of iterations, provide an onboard computation of the target states, executable for an uncoupled motion, and adjustable to various FWA and other unmanned aerial system platforms. An illustrative example is considered for a FWA maneuver in a vertical plane.

Keywords: Autonomy, path planning, navigation, guidance, control, hierarchical mixture of experts, instantaneous screw motion invariants.

Nomenclature

$\mathbf{a}$ - commanded thrust acceleration, $[m/s^2]$
$c_i,\ i = 1, ..., 6$ - integration constants
$C_L,\ C_D$ - aerodynamic lift and drag coefficients
$\mathbf{D},\ \mathbf{L}$ - aerodynamic drag and lift
$\mathbf{e}, \mathbf{e}_i^F\ (i = 1, 2, 3)$ - unit vectors of F-frame
g_{ik} - weights assigned by the gating network
g_0 - gravitational acceleration, $[m/s^2]$
$\mathbf{G}_g$ - gravity gradient vector
a_1 - difference between thrust component and aerodynamic drag accelerations, $[m/s^2]$
a_2 - acceleration due to thrust component and aerodynamic lift, $[m/s^2]$
H - Hamiltonian
h - vertical coordinate or altitude, $[m]$
m - mass, $[kg]$
S - FWA's effective area, $[m^2]$
t - time, $[s]$
$\mathbf{T}$ - thrust, $[N]$
v - magnitude of velocity vector, $[m/s]$
$\mathbf{W}$ - weight, $[kgm/s^2]$
$\mathbf{x}$ - state vector
α - angle of attack, rad]
$\bar{\alpha}$ - angle between thrust and velocity vector, $[rad]$
$\beta,\ \phi,\ \psi$ - sideslip, bank and heading (velocity yaw) angles respectively, $[rad]$
β_m - ballistic coefficient
$\boldsymbol{\epsilon}$ - commanded angular acceleration
γ - flight path angle, $[rad]$
$\boldsymbol{\lambda}$ - co-state vector
ρ - atmospheric density, $[kg/m^3]$
$\boldsymbol{\omega}$ - angular velocity vector, $[rad/s]$
$v_i,\ \omega_i$ - ISM invariants, $[m/s,\ rad/s]$
$\xi,\ \eta$ - horizontal coordinates, $[m]$

Introduction

Rapid advances in computing, robotics, sensors and control technologies drive the requirement to augment expensive manned systems with less expensive, unmanned and fully autonomous systems with many critical capabilities [1]-[3]. Numerous studies and experimentations have been dedicated to develop such capabilities as sense-and-avoid, autonomous selection of targets in real-time, guidance to a point on map if a communication with a ground-based pilot were lost [3]-[6]. Development of an onboard control system, consisting of an integrated guidance, navigation and con-

*Assistant Professor. 2540 Dole Street, Holmes 202A, Honolulu, HI, 96822. University of Hawaii at Manoa. Email: azimov@hawaii.edu.

†Graduate Student. 2540 Dole Street, Holmes 302, Honolulu, HI, 96822. University of Hawaii at Manoa. Email: evankawa@hawaii.edu

978-1-5386-1353-5/18/$31.00 ©2018 IEEE

trol (GNC) functions that can be executed in uncertain or unexpected circumstances is one of the key steps in leveraging the autonomy and enabling the unmanned aerial systems (UASs) with these capabilities [4]-[9]. Such systems include a fixed-wing aircraft, quadcopter, octocopter and other multi-rotor systems. In many studies, the GNC functions are considered error-free and computed separately for translational and rotational motions using pre-determined target states (or targets) [10],[11]. In this work, a target state means a state vector with desired components, although some of which may not be specified. As a result, the errors in the dynamical and measurement models for one (translational) motion are not coupled with those of the other (rotational) motion. Consequently, due to the accumulation of the errors inherited from the other motion, the efforts to separately compensate for such errors may not improve the overall accuracy and quality of real-time motion control. Such a decoupled treatment of the errors may not be significant in usual circumstances, but it may affect the quality and accuracy of guidance and control thereby negatively impacting the autonomy of the system [12].

Moreover, in unexpected circumstances, such as a flight in the vicinity of uncontrollable objects, where the accuracy of navigation (state and parameter estimation) schemes primarily designed for a traditional decoupled motion and availability of the correct target states for guidance performance become critical, the existing GNC functions may not perform in a satisfactory manner (Fig.1). To summarize, a complete real-time GNC system for an uncoupled motion of a single UAS in unexpected circumstances would be of interest to enable a UAS with the desired capabilities. This paper intends to create a framework with real-time and integrated GNC system for a fixed-wing aircraft (FWA). This framework can then be extended and adjusted to another platforms and types of UAS. It is known that the method of an Extended Kalman Filter (EKF)-based Hierarchical Mixture of Experts (HME) can provide highly accurate "offline" navigation solutions for an interplanetary orbit determination in uncertain environments [13], [14]. However, this method has not yet been associated with motion planning or control functions. Note also that both translational and attitude motions can be described by Hamiltonian equations, which in turn offer an opportunity to unify the motion analysis into one framework [15]. Finally, the previous studies of the authors have revealed an interesting advantage of using Giulio Mozzi's instantaneous screw motion (ISM) concept over the traditional decoupled motion dynamics for guidance and control [11], [15], [16]. That is the existing explicit expressions of the ISM invariants of a general 6-degrees-of-freedom (DOF) motion in terms of the decoupled motion parameters can be used to analytically compute the guidance commands without any iterative processes [7]. The authors' **objective** is to integrate three component-technologies, namely 1) Hamiltonian formalism-based motion planning framework, 2) the EKF-HME-based state and parameter estimation, and 3) the ISM invariants-based guidance with targeting capability into a unique and real-time GNC framework for a 6DOF motion of an autonomous FWA (Fig.1). This objective is accomplished by performing the following **primary research tasks**: 1) demonstrate new analytical and/or numerical trajectory and attitude solutions to FWA's equations of motion and their utility for motion planning; 2) establish a new, high-fidelity computational framework of a HME for an onboard state and parameter estimation utilizing sensor data fusion technology; and 3) create a target-relative guidance scheme utilizing the ISM invariants

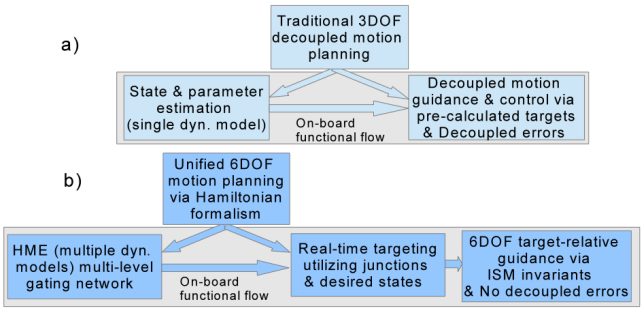

Figure 1: (a) Traditional functional block-diagram of UAS GNC system. (b) Proposed TGNC system.

Analytical Solutions for a Flight in a Vertical Plane

In this section the analytical solutions presented in [17] and [18]. Consider the following coordinate systems: the ground axes system, $Exyh$ fixed at the sea level; the local horizon axes fixed at the FWA center of gravity (COG); the wind axes system which also originates at the COG and the x-axis of which is aligned with velocity; and the body axes system fixed to the FWA (Fig.2). Then similarly to a conventional aircraft case, the equations of a FWA flight over a flat Earth with zero side slip angle, are [18]:

$$\begin{array}{ll} \dot{x} = v\cos\gamma\cos\psi, & \dot{v}a_2 - g_0\sin\gamma, \\ \dot{y} = v\cos\gamma\sin\psi, & v\dot{\gamma} = a_2\cos\phi - g_0\cos\gamma, \\ \dot{m} = -cT & v\dot{\psi} = a_2\sin\phi/\cos\gamma, \\ \dot{h} = v\sin\gamma, & a_1 = \frac{1}{m}(T\cos\bar{\alpha} - D)\ , \\ & a_2 = \frac{1}{m}(T\sin\bar{\alpha} + L) \end{array} \quad (1)$$

where $x,\ y,\ h$ are the coordinates of the FWA COG, v is the velocity, γ and ψ are the flight path angle (FPA) and heading angle, g_0 is the constant gravitational acceleration, c is a given constant, T is the thrust, m is the mass, $D = 0.5C_D\rho Sv^2$ is the drag, $L = 0.5C_L\rho Sv^2$

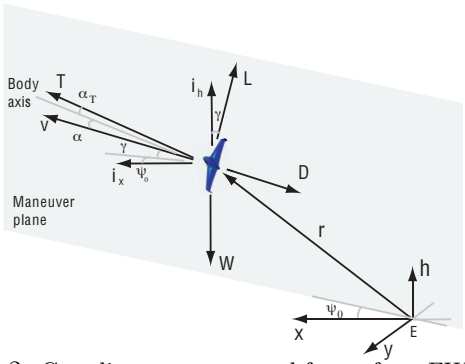

Figure 2: Coordinate systems and forces for a FWA flight.

is the lift, C_D and C_L are the drag and lift coefficients, ρ and S are the atmospheric density and the FWA's effective area, $\bar{\alpha} = \alpha + \alpha_T$ is the angle between the thrust vector and the velocity vector, and α is the angle of attack. Change of the FWA's mass is assumed negligible and therefore, $m = const$. It has been shown that if (a) accelerations due to the difference between thrust component and D, and the addition of the thrust component with L are not changed (a_1 and a_2 are constants), and (b) the bank angle is not changed ($\phi = \phi_0$), then Eqs.(1) are completely integrable in analytical functions and quadratures [19]. Note that the analytical integrability of Eqs.(1) in a closed-form is one of the important aspects of motion planning. Its complete integration reveals the general integral, which consists of four independent first integrals and two quadratures, including six independent integration constants. If $a = a_2,\ b = -g_0$, then the case with $a^2 \leq b^2$ corresponds to level flight, re-entry vehicle or missile dynamics, and Eqs.(1) can be integrated in quadratures [4], [19]. For the majority of problems of atmospheric flight mechanics, the lift acceleration is greater than the gravitational acceleration, that is $a^2 > b^2$, which will be considered below. In particular, if the heading angle is not changed ($\psi = \psi_0$), then under the assumptions (a,b), the FWA flight is confined to a vertical plane, and Eqs.(1) are completely integrable in analytical functions. Note that if ψ is a function of time, then Eqs.(1) are still integrable, and the flight trajectory is not confined to a vertical plane. One of the classes of analytical solutions and control laws for flight in a vertical plane can be presented as in Eqs.(2) [18].

$$
\begin{array}{ll}
x(\gamma) = P\cos\psi_0\exp(2z_1) + c_4, & \theta = \gamma + \frac{\pi}{2}, \\
y(\gamma) = P\sin\psi_0\exp(2z_1) + c_5, & z_1 = \frac{2A}{d_1}\times \\
h(\gamma) = Q\exp(2z_1) + c_6, & \arctan\frac{a\tan(\theta/2)+b}{d}, \\
P = P(\theta),\ Q = Q(\theta) & p_1 = \frac{c_2}{A^2+a^2-b^2}, \\
v(\gamma) = c_2 z_2\exp(z_1), & z_3 = \frac{A+b\cos\theta}{a+b\sin\theta} + \frac{a}{A}, \\
t(\gamma) = p_1\exp(z_1)z_3 + c_3, & z_2 = (a+b\sin\theta)^{-1}, \\
\psi(\gamma) = \tan\phi_0 z_4 + c_1, & z_4 = \ln(\tan(\theta/2)) + \\
s_1 = ma_1 + D & g_0 z_1/a_1, \\
s_2 = ma_2 - L & \tan\bar{\alpha}(h,v) = \frac{ma_2-L}{ma_1+D}, \\
T(h,v) = \sqrt{s_1^2+s_2^2}, &
\end{array}
\tag{2}
$$

Here $\sin\theta \neq -1$, and $c_2,\ d,\ A = a_1,\ a = a_2,\ b = -g_0$ are the integration constants. T and α can be considered as the control parameters (Fig.6). The solutions in Eqs.(2) are used to compute the new target states and initialize a new plane of flight. These states are computed as the state vectors consisting of the desired position, velocity and time. The constants $c_1,\ c_2, ..., c_6$ can be computed using the initial conditions of flight. This approach to motion planning and targeting is critical to the FWA's autonomy, and is used in the proposed control framework.

Targeting and GNC Functions

This section describes each of the three component-technologies, namely, the Hamiltonian formalism-based motion planning, the HME- based state estimation, and the ISM invariants-based guidance with their primary research tasks to construct the proposed GNC framework with the target-relative guidance system synthesis.

Framework for Motion Planning

Motion planning describes trajectory and attitude profiles, which satisfy the equations of motion, terminal conditions, and state and control constraints (Fig.2). One can show that the equations of motion of an aircraft, including Eqs.(1), can be presented in a canonical form: $\dot{\mathbf{x}} = [\partial H/\partial\boldsymbol{\lambda}]^T$, $\dot{\boldsymbol{\lambda}} = -[\partial H/\partial\mathbf{x}]^T$, where $\mathbf{x}$ and $\boldsymbol{\lambda}$ are the state and co-state vectors, and H is the Hamiltonian [20]. The state vector will be defined as $\mathbf{x} = \mathbf{x}(\mathbf{r}, \mathbf{v}, \boldsymbol{\eta}, \boldsymbol{\omega}, \mathbf{p}, m)$, where the arguments are position, velocity, angle and angular rate vectors, a vector of estimate parameters, and mass respectively. Since these equations are valid separately for point mass and attitude motions, they allow for a unified framework of motion planning using the Hamiltonian formalism [15]-[20]. There exist many powerful state-of-the-art

programs of numerical integration of equations (SORT, GMAT, POST, etc.) and the methods of analytical dynamics (Levi-Civita, Noether, Lee, Poisson, Poincare, Hamilton-Jacobi, etc.) developed for analytical integration of the canonical equations [10], [21]. For the last two decades, many studies have also been devoted to explore other aspects of motion planning, including controllability, kinematic and tactical constraints, and the real-time implementation [22], [23]. In particular, the studies of dynamics of Dubins airplane, and vertical takeoff and landing (VTOL) maneuvers have revealed many interesting features of the UAS flight, such as the utility of waypoints or desired points under simplified assumptions [23]. Moreover, the authors' studies have shown that the spacecraft, lander and aircraft trajectories can be analytically synthesized using the junction (desired, target or waypoint) points, which are designated in real-time and can be used as the guidance targets [24]. This paper demonstrates that, as an analogy between these flight vehicles' and the FWA dynamics, this concept of utility of the target states, which are analytically (or numerically)- computed on-board in real-time (real-time targeting), can also be used for guidance and control. So, derivation of general or even particular analytical solutions becomes an important problem of controllable motion.

Framework for HME Performance

The EKF-HME-based state and parameter estimation component-technology is based on the framework of the HME, regulated by multi-level gating networks providing highly accurate onboard navigation solutions in real-time (Fig. 3). **Hierarchical Mixture of Experts**. The HME is an approach for a state and parameter estimation, and was successfully used for an interplanetary orbit determination in the presence of uncertainties, such as turbulence or uncounted perturbations [13]. For a given vector of measurements and for a given time, the HME executes banks of experts (EKFs) with low- and top-level gating networks to optimize the best state and parameter estimates [25]. As a structure, a mixture-of-experts (ME) belongs to a class of neural network models that are inspired by mixture models from statistics [26]. In the last decade, the modular adaptive Kalman filtering using the ME - framework, regulated by a gating network, opened various possibilities to develop high-accuracy adaptive estimation procedures and multi-sensor fusion techniques [13], [28]. The implementation of the ME methods are mainly associated with an EKF bank approach, which deals with uncertainties in the dynamics models, such

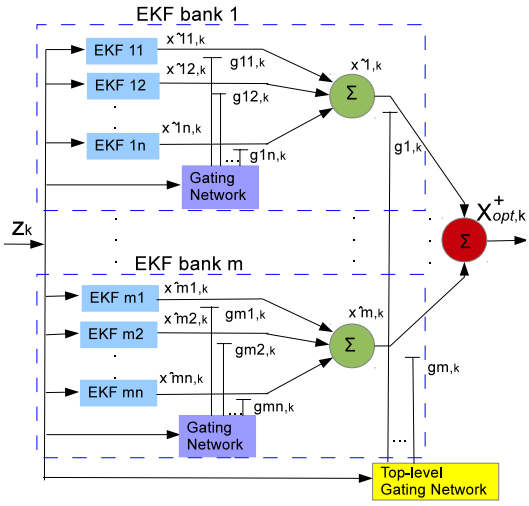

Figure 3: Proposed EKF-HME with multilevel gating network architecture to provide optimal estimate $\hat{\mathbf{x}}^{+}_{opt,k}$.

as Dubins airplane model, and the estimate parameters [27]-[29]. The proposed HME structure embeds sensor data fusion technology and a finite number of HMEs with their EKF banks (elements) running in parallel. Each HME provides its own representation of the estimated state and parameters with a low-level gating network. A weighting function is then applied to each filter bank output to find the best performing filter utilizing a top-level gating network. In the proposed work, the data collected by FWA sensors are fused through processing by multiple EKF banks, regulated by a low- and top-level gating networks (Fig.3). In this fusion, all filters of the gating network bank compete to be selected as the best performing filter. The EKF-HME has flexibilities in the number of dynamic models and in estimate parameters, such as atmospheric parameters, drag and lift coefficients. A FWA autonomy can be improved, in particular, by accommodating different models and parameters, data fusion, and switches between various filters thereby better accounting for the uncertain conditions. Furthermore, since the HME has inherent parallel architecture, the proposed work will provide a fully parallel and scalable computational methodology for an onboard state and parameter estimation.

Guidance via Instantaneous Screw Motion Invariants

The ISM invariants-based guidance component- technology is based on the utility of the motion planning and state estimation technologies, and represents extension and modification of the mission-proven guidance technology.

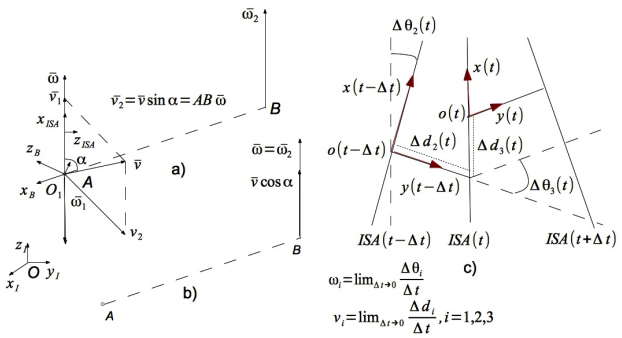

Figure 4: (a,b) Definition of ISA. c) The ISA at three consecutive time instances [11].

Instantaneous Screw Motion and its Invariants. Unlike the traditional representation of a motion in terms of decoupled translation and rotation, in 1763 Gulio Mozzi proved that **any full rigid body motion can be described by an instantaneous screw axis** [31] (Fig.4). If $\bar{\boldsymbol{\omega}}$ and $\bar{\mathbf{v}}$ the angular velocity of a rigid body motion and the translational velocity of its given point (*kinematic twist*), and $\delta = (\bar{\boldsymbol{\omega}}, \bar{\mathbf{v}})$, then this motion with respect to an inertial $Ox_Iy_Iz_I$-frame or a body $O_1x_By_Bz_B$-frame can be characterized by an instantaneous translational motion with velocity $\bar{v}_2 = \bar{\mathbf{v}} \sin\delta$ along an ISA and an instantaneous rotational motion with velocity $\bar{\boldsymbol{\omega}}_2 = \bar{\boldsymbol{\omega}}$ about the same axis displaced at a distance AB from the given point. Here the ISA-frame is attached to the ISA axis. Fig.4 illustrates instantaneous translational (Δd) and rotational ($\Delta\theta$) displacements which form six unique, coordinate-free, time-based ISM invariants, ω_i and v_i, $i = 1, 2, 3$ [11]:

$$\omega_i(t) = \omega_i(\boldsymbol{\omega}, \dot{\boldsymbol{\omega}}, \ddot{\boldsymbol{\omega}}), \quad v_i(t) = v_i(\mathbf{v}, \dot{\mathbf{v}}, \ddot{\mathbf{v}}, \boldsymbol{\omega}, \dot{\boldsymbol{\omega}}, \ddot{\boldsymbol{\omega}}), \quad (3)$$

where $\dot{\boldsymbol{\omega}} = (\boldsymbol{\omega}, \boldsymbol{\tau})$, $\ddot{\boldsymbol{\omega}} = \ddot{\boldsymbol{\omega}}(\boldsymbol{\omega}, \boldsymbol{\tau}, \dot{\boldsymbol{\tau}})$, $\dot{\mathbf{v}} = \dot{\mathbf{v}}(\mathbf{v}, \mathbf{u})$ and $\ddot{\mathbf{v}} = \ddot{\mathbf{v}}(\mathbf{v}, \mathbf{u}, \dot{\mathbf{u}})$ according to dynamics equations. Once $\mathbf{u} = \mathbf{u}(\mathbf{x}, \mathbf{p}, t)$ and $\boldsymbol{\tau} = \boldsymbol{\tau}(\mathbf{x}, \mathbf{p}, t)$ are obtained from the motion planning solutions, and Eqs.(3) are used to compute nominal ω_i and v_i.

Real-time targeting and re-targeting. The real-time targeting is proposed as a key function to leverage the FWA autonomy and therefore, it is part of the proposed guidance component-technology (Fig.5). It consists of onboard computations of the target states and nominal time to achieve the target. The proposed research introduces guidance (G) and platform (P) frames as shown in Ref.[24]. The P-frame is a fixed frame, and its P origin coincides with the E origin of the $Exyh$-frame, and the X_pZ_p-plane of the P-frame coincides with the maneuver plane, which forms the angle ψ_0 with the xh-plane (Fig.2). At anytime, $t \geq t_0$, the X_pZ_p-plane (or the maneuver plane) will contain the E origin of the $Exyh$-frame, the FWA's COG and the nominal target thereby forming the (current) maneuver plane of the nominal trajectory. In contrast,

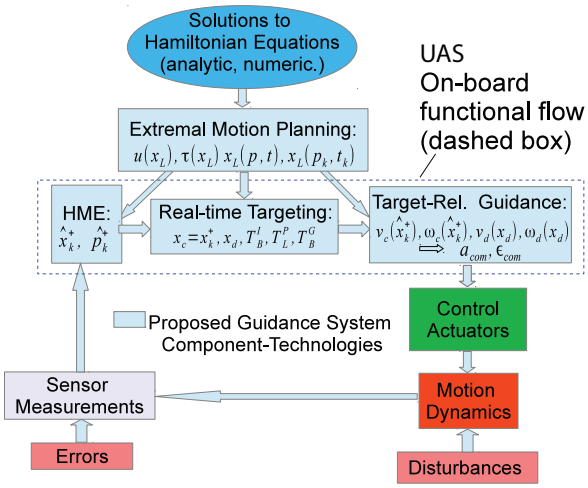

Figure 5: Proposed guidance system synthesis.

at any time, the origin of the G-frame coincides with the target. The target state may be changed, in particular, to avoid a collision with a flying or stationary object, or to re-orient the FWA. The integration constants of the solutions will change due to the change in the target point, thereby changing the X_pZ_p-plane (the xh-plane) of the maneuver, and thus, yielding a new re-targeted trajectory. That is, this plane can be seen as a dynamical plane, which oscillates each time when re-targeting is performed (Fig.5).

Guidance laws. The *original and general concept of guidance*, known as the explicit (E)-guidance, was developed first by George Cherry, and then modified by Alan Klumpp to formulate quartic polynomial-based lunar descent guidance, which was implemented in all Apollo missions [30]. The thrust acceleration to be commanded at any point in space consists of three terms: the acceleration of the reference trajectory at a particular time, minus two feedback terms proportional to velocity and position deviations from the reference trajectory. Since 1970's, a wide range of guidance and feedback control schemes have been developed and tested for the FWAs. In particular, Lyapunov's second and vector fields' methods, the **v**-nulling method, the guidance schemes based on proportional navigation, path-following, predictive control, line of sight, vision, sliding mode, and other numerical, approximate and analytical methods [32]-[39]. In most cases, these guidance schemes rely on approximate solutions, and the guidance targets are considered as predetermined inputs [9]. This work proposes new analytical scheme, a modification of the E-guidance, to compute the commanded accelerations using the differ-

ences of the ISM invariants' current and desired values:

$$\mathbf{a}_{com} = \mathbf{c}_1(\mathbf{x}_c, \mathbf{x}_d, t_c, t_d)p_1(v_{ic}, \omega_{ic}, v_{id}, \omega_{id}) +$$
$$\mathbf{c}_2(\mathbf{x}_c, \mathbf{x}_d, t_c, t_d)p_2(v_{ic}, \omega_{ic}, v_{id}, \omega_{id}) - \mathbf{g},$$
$$\boldsymbol{\epsilon}_{com} = \mathbf{c}_3(\mathbf{x}_c, \mathbf{x}_d, t_c, t_d)p_3(\omega_{ic}, \omega_{id}) +$$
$$\mathbf{c}_4(\mathbf{x}_c, \mathbf{x}_d, t_c, t_d)p_4(\omega_{ic}, \omega_{id}) - \Omega \times \mathbf{I}\Omega - \mathbf{G}_g, \qquad (4)$$

where $\Omega = (\omega_x, \omega_y, \omega_z)$, $\mathbf{I} = (I_x, I_y, I_z)$ and $\mathbf{G}_g$ is the gravity gradient vector, and note that $\mathbf{c}_i$ and p_i, $(i = 1, ..., 4)$ incorporate the errors of the decoupled motions. Subject to further studies are the techniques of computing the guidance functions based on other guidance methods, including the Lyapunov's second methods using the ISM framework.

Illustrative Examples

Example 1: Simulations of Flight in a Vertical Plane.

As an illustrative example of the proposed framework component-technologies, a set of simulations of a wide range of climb maneuver trajectories of a small FWA in a vertical plane for various flight parameters and terminal conditions has been performed according to the solutions in Eqs.(2). The computations of the solutions have been conducted in accordance to Ref.[18] (see Fig.6). The inputs used are $t_0 = 0.0$, $g_0 = 9.8$, $b = -9.8$, $\Delta\gamma = 20$, $\rho_0 = 20.0$, $h_0 = 10.0$, $\psi_0 = 0$, $\varphi_0 = 0$, $a_2 = A = 0.1$, $a_2 = a = \sqrt{b^2 + k^2}$, $k \in [5 - 100]$, $m \in [30 - 100]$ lbs/g_0, $v_0 = [50 - 125]$ m/s, $\gamma_0 \in [0,\ 20^o]$, The flight path angle, γ is considered as an independent variable. In particular, the computations have shown that the magnitude of velocity on the climb trajectories is a decreasing function of time, although it is sensitive to changes in A, a and W (Fig. 7). As $A = const$, the thrust, T is a decreasing function of t, and an increasing function of v. The results also show that higher v_0's and/ or larger differences between the initial and final γ's yield longer flight times. Changes in S do not impact the relationships between the rate of climb, $\dot{h}$ and v, between v and t, and between h and v. These changes, however, do impact the relationships of α and T with v. Also, changes in m do not impact T and α profiles significantly. This example, in particular, demonstrates that the analytical solutions in Eqs.(2) reveal interesting qualitative features of the FWA nominal trajectories, and can be used for tracking purposes.

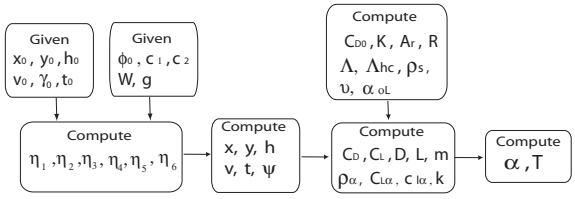

Figure 6: Flow chart of computations of control functions.

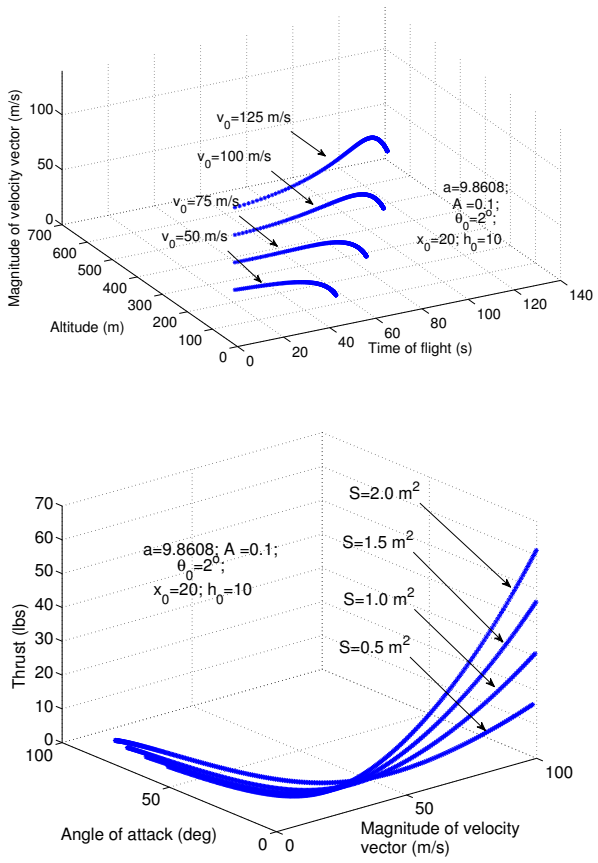

Figure 7: Time vs velocity and altitude for various v_0. Lower: Velocity vs thrust and angle of attack for S.

Example 2: Guidance System Performance.

This example illustrates the performance of the proposed GNC framework and its advantages over the existing FWA control systems (Fig.1). For simplicity, a climb maneuver in a vertical plane is considered (see Example 1 above). The FWA parameters, the initial position and covariance, process- and measurement noise matrices are given in Table 1. It is assumed that the ground radar measures the FWA altitude, h, and the observer radar measures the range, r from the origin of the $Exyh$ system to the FWA COG (see Fig.2). **Task 1: Motion planning**. The climb maneuver with duration $t_f = 110.7$ sec. is simulated using the

solutions in Eqs.(2) (Fig.8).

Task 2: Estimation. The EKF-HME has been created with 2 banks (B1,B2), each of which consists of 4 EKFs (E1-E4) and is outlined in Table 2. The nominal EKF (E1) uses the analytical solutions given in Eqs.(2) for the state propagation. For simplicity, the state $\mathbf{x} = \mathbf{x}(x,\ y,\ h,\ \dot{x},\ \dot{y},\ \dot{h},\ m,\ C_D)$ is assumed affected ("perturbed") by a random process noise and scale factor errors. The process noise and measurement noises are given with zero mean and their covariance matrices Q and R. The uncertainty covaraince is given by $p_{ii},\ i = 1, ..., 8.$ r, as a measurement function, can be computed using $h,\ x,\ y$ and ψ_0. Figures 8 and 9 show that for those EKFs that use the radar measurements, the combined RMS position and C_D estimates' errors are smaller than those from different EKFs, except for the observer radar and scaled perturbed state cases. It has been shown that the RMS errors are very sensitive to the changes in scaling coefficients and therefore, these changes are subject to tuning of these coefficients. These figures demonstrate that combined RMS errors computed using EKF-HME estimates are more accurate compared to individual EKFs. This result holds if the number of banks of HME is increased.

Task 3: Guidance. Tasks 1 and 2 have been used to compute commanded thrust acceleration, $\mathbf{a}_{com}$, thereby synthesizing the guidance system. For simplicity, no commanded angular acceleration, $\boldsymbol{\epsilon}_{com}$ was computed during the maneuver. As expected, Fig.10 (lower), shows that the ISM invariants, with the translational and attitude errors incorporated, behave closely to their nominals during the maneuver except for the last several seconds, at which singularities occur in the analytical solutions. These cases of singularities are subject to more detailed analysis during the project period. This figure also shows that the deviations between the current and desired ISM invariants are decreasing over time on all axes as expected. Fig.10 (upper) shows that $\mathbf{a}_{com}$ is correctly guiding the FWA along the trajectory while counting for the attitude changes via the ISM invariants. This example demonstrates that compared to the nominal analytical solutions for a decoupled motion, the proposed control framework with guidance system synthesis 1) treats a 6DOF motion and its errors without its decoupling, 2) counts simultaneously for various uncertainties in the multiple dynamic models, including wind, and 3) provides a better estimation and guidance through EKF-HME and non-iterative analytical computations, thereby making a step forward towards the FWA autonomy. The proposed GNC framework is robust in terms of the shape or type of the maneuver trajectory, and consequently, can be used for other types of flight maneuvers.

Estimated CPU Time for the Guidance Computations. Given 110.7 seconds of flight time in the "Example 2" above, the CPU (Central Processing Unit) times spent for the guidance computations were in total 3.11, 4.55 and 6.76 seconds including the processing of 100, 200 and 300 measurements respectively. This would indicate that for each cycle of measurements the proposed system can be executed onboard instantly.

Table 1. Example 2: UAS parameters, initial position and covariance, process- and measurement noise matrices

$I_x = 8$	$I_y = 5$
$I_z = 3$	$W = 3.64$
	$S = 0.5$
$x_0 = 20$	$y_0 = 0$
$h_0 = 10$	$v_0 = 100$
	$\theta_0 = 2^o$
$p_{11} = 0.8147$	$p_{22} = 0.1201$
$p_{33} = 0.1397$	$p_{44} = 0.3118$
$p_{55} = 0.6324$	$p_{66} = 0.2785$
$p_{77} = 0.0975$	$p_{88} = 0.1270$
$Q(1,1) = 0.9755$	$Q(2,2) = 0.0012$
$Q(3,3) = 0.0012$	$Q(4,4) = 0.0014$
$Q(5,5) = 0.4883$	$Q(6,6) = 0.0194$
$Q(7,7) = 0.01801$	$Q(8,8) = 3.4440$
$\mathbf{R}_{1,meas} = \sigma_1^2 = 5.1221$	$\mathbf{R}_{2,meas} = \sigma_2^2 = 1$

Table 2. Example 2: EKF-HME bank experts. Inputs: $\mathbf{x}_L,\ \beta,\ \mathbf{P}_0,\ \mathbf{Q},\ \mathbf{R}_{meas}$. Outputs: $\hat{\mathbf{x}}^+_{opt,k},\ \hat{C}^+_{D-opt,k}$.

(E1,B1): Nom. EKF, gr. rad	(E5,B2): Pert. $\mathbf{x}$, GEO obs.
(E2,B1): Pert. $\mathbf{x}$, gr. rad	(E6,B2): Pert. $\mathbf{x}$, gr. radar, C_D est.
(E3,B1): Iter. EKF gr. rad	(E7,B2): Pert. state, obs. radar, C_D est.
(E4,B1): Sc.-pert. $\mathbf{x}$, gr. rad	(E8,B2): Sc.-pert. $\mathbf{x}$, obs. radar, C_D est.

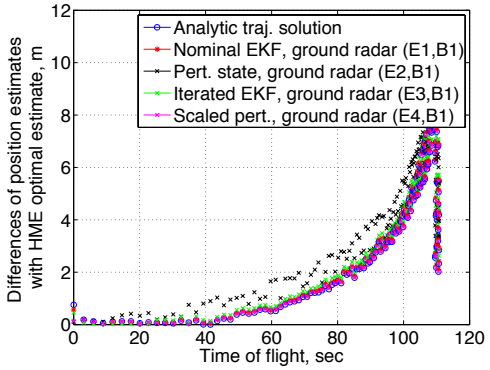

Figure 8: Differences of HME's estimates.

Relations to Current Flight Software

Most recent GNC UAS development used ArduPilot or PX4 [40]. Typically, the Pixhawk flight controller is used, which has an update rate of 400 Hz. Beall's adaptive flight controller's performance and adaptation gain

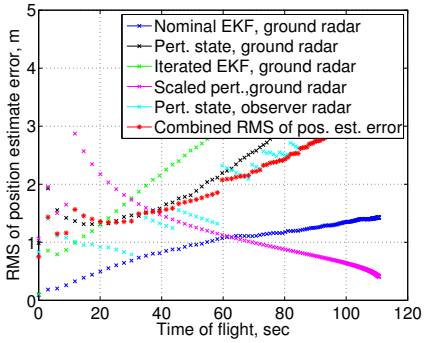

Figure 9: Combined RMS: position error.

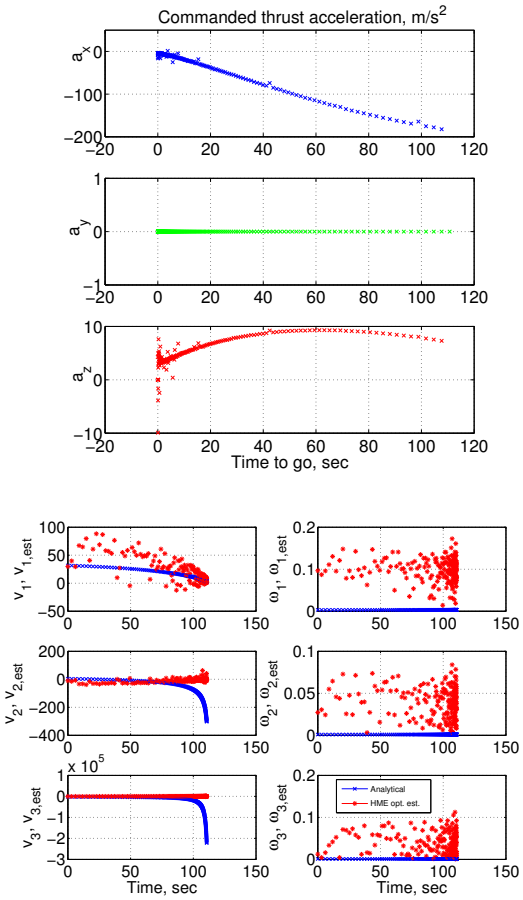

Figure 10: Commanded thrust acceleration vs time to go. Below: ISM parameters' estimates for HME.

are maximized as the update rate increases, i.e. dt approaches zero. Therefore, higher update rates increase performance [41]. To the authors' current knowledge, there are not any recent GNC UAS development in flight software, known as INAV since most development has been done in ArduPilot or PX4. Changing INAV's current structure to match the proposed guidance system synthesis will fulfill the proposed tasks of integrating Hamiltonian formalism-based motion planning framework, EKF-HME-based state and parameter estimation, and ISM invariants-based guidance into an autonomous FWA (Fig. 5, 11).

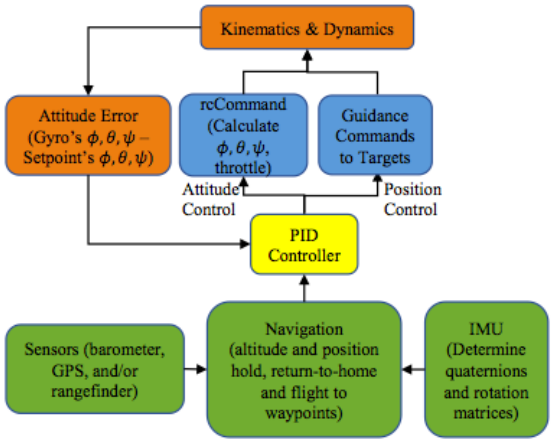

Figure 11: INAV Architecture

Conclusions

The real-time GNC framework for UAV maneuvers in a vertical plane has been developed. This framework represents the integration of the three component- technologies, consisting of the Hamiltonian formalism-based motion planning framework, the EKF-HME- based state and parameter estimation, and the ISM invariants-based guidance with targeting capability. Due to canonical equations of the motion planning and the ISM invariants, the proposed framework can be implemented for a 6DOF motion. The performance of the proposed framework has been illustrated with the example of a climb maneuver, including the computations of the motion planning solutions, the estimation procedures and the guidance command computations thereby demonstrating the real-time guidance system synthesis. The future studies include modification of the proposed GNC framework to facilitate more on-board capabilities, including the generation of the maps of areas of interest and "sense and avoid" capability for beyond-line-of-sight maneuvers.

References

[1] Making Way for Unmanned Aircraft. *Aerospace America*. 2013, July-August, N.1, pp.29-31.

[2] R. W. Beard and T. W. McLain. Small Unmanned Aircraft: Theory and Practice. Princeton Universitty Press, Princeton, NJ, 2012, 320 pp.

[3] Eaton, C.M., Chong, EK.P., and Maciejewski, A.A. "Multiple-Scenario Unmanned Aerial System Control: A Systems Engineering Approach and Review of Existing Control Methods", *Aerospace*, 2016, V.3, N.1. doi:10.3390, 26 p.

[4] Ralston, T. and Azimov, D.M. Integrated Onboard Sensor Fusion, Targeting, Guidance and Control Framework for Autonomous Unmanned Aerial Systems. September 1, 2015. Alaska UAS Interest Group 2015. Annual Meeting. Fairbanks, AK. 13 p.

[5] Yu, X. and Zhang, Y. Sense and Avoid Technologies with Applications to Unmanned Aircraft Systems: Review and prospects. *Progress in Aerospace Sciences*. 2015, N. 74, pp. 152?166.

[6] Handbook of Unmanned Aerial Vehicles. Editors: K. Valavanis, George J. Vachtsevanos. 2015. Springer Netherlands. 3022 p.

[7] Azimov, D.M. Analytical Synthesis of Optimal Trajectory Control and Guidance Solutions With Applications to Autonomous Systems. The 46th ISCIE International Symposium on Stochastic Systems Theory and Its Applications (SSS 2014). October 31- November 2, 2014. Kyoto. Japan.

[8] Azimov, D.M. Analytical Methods of Synthesis of Optimal Trajectories for On-board Guidance. Abstract of Dissertation for Degree of "Doctor of Sciences" in *Dynamics, Ballistics and Flight Vehicle Control*. Moscow Aviation Institute. Moscow Aviation Institute Press. Moscow, Russia. October 25, 2007, 35 p.

[9] Lin, C.F. Modern Navigation, Guidance and Control Processing. Prentice Hall, Englewood Cliffs, New Jersey, 1991. 671 p.

[10] Whittaker, E. T., *A Treatise on the Analytical Dynamics of Particles and Rigid Bodies*, 5th Edition, University Press, Cambridge, UK, 1985.

[11] Schutter, J.D. "Invariant Description of Rigid Body Motion Trajectories", *Journal of Mechanisms and Robotics*. 2010, V.2, pp. 011004-1-011004-9.

[12] Garcia, C., Lozano, P., Dzul, R., Enrique, A. Modeling and Control of Mini-Flying Machines. 2005. Advances in Industrial Control.

[13] Chaer, W.S., Bishop, R.H., Ghosh, J. "A Mixture of Experts Framework for Adaptive Kalman Filtering," *IEEE Transactions on Systems*, Man, and Cybernitics, V.27, N.3, June 1997, pp.452-464.

[14] Rao, A.J., Miller, D., Rose, K., Gersho, A. "Mixture of Experts Regression Modeling by Deterministic Annealing," *IEEE Transactions on Signal Processing*, V.45, N.11, November, 1997, pp. 2811-2820.

[15] Junkins, J.J. How Nonlinear Is It? A Tutorial on judicious Coordinates for Orbit and Attitude Dynamics. Paper AAS 03-286. John L. Junkins Astrodynamics Symposium. College Station, TX. 23-24 May, 2003, pp.1-23.

[16] Angeles, J. "Automatic Computation of the Screw Parameters of Rigid-Body Motions. Part II. Infinitesimally- Separated Positions," *ASME Journal of Dynamical Systems, Measurements and Control*. 1986, V.108, pp. 39-43.

[17] Azimov, D.M. and Allen, J. Analytical Model and Control Solutions for Unmanned Aerial Vehicle Maneuvers in a Vertical Plane. ICUAS 2017. Final Program and Book of Abstracts. June 13-16, 2017, p.77.

[18] Azimov, D.M. and Allen, J. Analytical Model and Control Solutions for Unmanned Aerial Vehicle Maneuvers in a Vertical Plane. *Journal of Intelligent and Robotic Systems*. DOI 10.1007/s10846-017-0669-4. Springer Science+Business Media B.V. 2017. Accepted for publication on 30 June 2017. 9 p.

[19] Azimov, D.M. "On One Case of Integrability of Atmospheric Flight Equations", AIAA *Journal of Aircraft*. 2011, V.48, N.5, pp.1722-1732.

[20] Vinh, N. X., Optimal Trajectories in Atmospheric Flight. Elsevier, Amsterdam, 1981, pp. 7?20.

[21] Programmer's Guide for the Simulation and Optimization of Rocket Trajectories (SORT) Program. Version 7. Lockheed Engineering & Sciences Company. LESC-30423. Houston, Texas. October 1992.

[22] Yang, G. and Kapila, V. Optimal path planning for unmanned air vehicles with kinematic and tactical constraints. In Proceedings of the IEEE Conference on Decision and Control, pages 1301?1306, Las Vegas, NV, 2002.

[23] Hanson, C., Richardson, J., and Girard, A. Path planning of a Dubins vehicle for sequential target observation with ranged sensors. In Proceedings of the American Control Conference, pages 1698?1703, San Fran- cisco, CA, June 2011.

[24] Azimov, D.M. Real-Time Guidance, Control and Targeting Algorithms for Autonomous Planning and Execution of Space Operations. The 45th ISCIE International Symposium on Stochastic Systems Theory and Its Applications. November 1-2, 2013. University of Ryukyus, Japan.

[25] Azimov, D.M. and Bishop, R.H. An Overview of Mixture of Experts Structure and Gating Network Characteristics. Technical Report. UT-GNC-TR-12-06-5. The University of Texas at Austin. December 16, 2006. Austin, TX. 24 p.

[26] Jacobs, R.A. and Jordan, M.I. "Learning piecewise control strategies in a modular neural network architecture," *IEEE Transactions in Systems*, Man and Cybernetics, V.23, 1993, pp.337-345.

[27] Magill, D.T. "Optimal adaptive estimation of sampled stochastic processes," *IEEE Transactions on Automatic Control*, V.AC-10, October, 1965, pp.434-39.

[28] Bristeau, P.J., Callou, F., Vissiere, D., Petit, N. The Navigation and Control Technology Inside the AR.Drone Micro UAV. Preprints of the 18th IFAC World Congress Milano. Italy. August 28-September 2, 2011, pp.1477-1484.

[29] Anderson, R. and Milutinovic, D. A stochastic approach to Dubins feedback control for target tracking. In Proceedings of the IEEE/RSJ International Conference on Intelligent Robots and Systems, San Francisco, CA, September 2011.

[30] Klumpp, A.R. "Manually Retargeted Automatic Landing System for the Lunar Module (LM)", *Journal of Spacecraft and Rockets*. February, 1968.

[31] Ceccarelli, M. Screw axis defined by Giulio Mozzi in 1763. Proceedings of the Ninth World Congress on the Theory of Machines and Mechanisms (IFToMM). August 29-September 2, 1995. V.4, pp.3187-3190.

[32] Kelley, H. J. "Guidance Theory and Extremal Fields," *IEEE Transactions on Automatic Control*, 1962, pp.75-82.

[33] Huili Yu, H. and Beard, R.W. "A vision-based collision avoidance technique for micro air vehicles using local-level frame mapping and path planning", *Autonomous Robots*, 2013, V. 34(1-2), pp.93?109.

[34] Jensen, E. and Pfister, L. The Airborne Tropical TRopopause EXperiment (ATTREX). NASA Ames Research Center. espo.nasa.govmissionsattrex, 15 p.

[35] Sujit, B.J., Saripalli, S., Sousa, J.B. "Unmanned Aerial Vehicle Path Following: A Survey and Analysis of Algorithms for Fixed-Wing Unmanned Aerial Vehicles", *IEEE Control Systems*, V. 34, pp. 42-59. Online publication date: 1-Feb-2014.

[36] Yamasaki, T., Balakrishnan, S., Takano, H.. 2012. Separate-Channel Integrated Guidance and Autopilot for a Path-Following UAV via High-Order Sliding Modes. AIAA Guidance, Navigation, and Control Conference. August 13-16, 2012. Minneapolice, MN. AIAA 2012-4457.

[37] Al-Hiddabi, S., Shen, J. N.H. McClamroch. A study of flight manoeuvres for the PVTOL aircraft model. Proceedings of the 1999 American Control Conference (Cat. No. 99CH36251), 2727-2731.

[38] Cho, N., Kim, Y., Park, S. "Three-Dimensional Nonlinear Differential Geometric Path-Following Guidance Law", *Journal of Guidance, Control, and Dynamics*, V. 38, N.12, pp. 2366-2385.

[39] Gavilan, F., Vazquez, R., Camacho, E.F. " An iterative model predictive control algorithm for UAV guidance", *IEEE Transactions on Aerospace and Electronic Systems*, 2015, V.51, N.3, pp. 2406-2419. Online publication date: 1-Jul-2015.

[40] De Mel, D. H. S., Stol, K. A., Mills, J. A. D., and Eastwood, B. R. Vision-Based Object Path Following on a Quadcopter for GPS-Denied Environments. 2017 International Conference on Unmanned Aircraft Systems (ICUAS). Miami, FL. 13-16 June 2017, p. 2.

[41] Beall, R. G. Engineering of Fast and Robust-Adaptive Control for Fixed-Wing Unmanned Aircraft. Naval Postgraduate School. June 2017. pp.19-20